



# Numerical study of a wake-stabilized propane flame in a cross-flow of air



Alechenu A. Aboje, Kevin J. Hughes<sup>\*</sup>, Derek B. Ingham, Lin Ma, Alan Williams, Mohamed Pourkashanian

Energy Technology and Innovation Initiative, Faculty of Engineering, University of Leeds, Leeds LS2 9JT, UK

## ARTICLE INFO

### Article history:

Received 13 February 2015  
Received in revised form  
4 September 2015  
Accepted 6 September 2015  
Available online 9 October 2015

### Keywords:

Cross-flow diffusion flame  
Wake-stabilized flame  
Non-premixed model  
Partially premixed model

## ABSTRACT

Predictions of flame structures, flame temperatures, and species concentrations have been numerically performed for a wake-stabilized propane flame in a cross-flow of air. The flow field has been modeled using the Reynolds-Averaged Navier-Stokes equation incorporating the Reynolds Stress turbulence closure Model (RSM) and the Large Eddy Simulation (LES) technique with the two methods compared. The combustion processes were modeled using the partially premixed and the non-premixed models and the two sets of results have also been compared. The CRECK reaction mechanism was used to model the kinetics of the propane reactions while soot in the flame was modeled with the Moss-Brookes-Hall model. Thermal radiation in the flame was modeled with the discrete ordinate method. The results of the simulation have been validated against experimental data and show that the partially premixed model performs better than the non-premixed model for wake-stabilized flames that are attached to the lee-side of the flare burner. Furthermore, the LES technique has been shown to perform better than the RSM.

© 2015 Energy Institute. Published by Elsevier Ltd. All rights reserved.

## 1. Introduction

Environmental pollution associated with the flaring of hydrocarbon fuels has received much attention over the last few decades and most of this knowledge has been obtained from experimental studies on the laboratory scale [1,2]. This has resulted from the difficulties associated with the investigation of the full scale flares, however some work on full scale flares has been undertaken and the results from these investigations now form a central policy of the Environmental Protection Agency (EPA) on gas flaring [3]. Extensive research on full scale flares has also been performed by the Alberta Research Council (ARC) and the results of this research has helped to establish the significance of crosswinds on flare efficiencies, a factor which was not included in the EPA research [4]. On the laboratory scale, researchers have been able to probe the characteristics of flare-related diffusion flames more closely. Relationships between flame lengths and pipe internal diameters for different fuels have been established and the stability of propane flames in still air and in a cross flow of air have been investigated and reported [5,6]. Gollahalli and Nanjundappa [7] investigated propane flames in a cross-flow of air for various jet-to-cross flow momentum ratios that are related to gas flares, where they described the flow processes that control the mixing in the flame, namely a standing vortex trapped at the lee-side of the fuel pipe in the wake-stabilized regime and a pair of counter-rotating vortices downstream of the flame in a momentum-dominated regime. Huang et al. [8–10] also performed detailed experimental work on propane flames in a cross flow of air. They investigated the structure of the flames in various regimes as well as the species concentration and thermal field of the flames. They reported that for many hydrocarbon fuels, the burner-detached or lifted flame will only survive at cross-flow velocities lower than about 8 m/s while the attached flames can survive at much higher velocities. However, it has been observed that the burner tips tend to deteriorate more rapidly when flames are attached than when they are lifted due to the high temperatures at the burner tip. They also reported that if the flame was lit at a cross-flow velocity higher than a critical value, then the flame base could never leave the burner before blow-off, i.e. the flame will always attach to the burner on the leeside.

<sup>\*</sup> Corresponding author.

E-mail address: [K.J.Hughes@leeds.ac.uk](mailto:K.J.Hughes@leeds.ac.uk) (K.J. Hughes).

In recent years, computational fluid dynamics studies have been made of these flames and a large body of literature is available on the simulation of methane-air flames for both straight jets and to a less extent cross-flow flames. Notable among these is the work of Escudier [11] who investigated and predicted major and minor species in methane-air flames. Castiñeira and Edgar [12] performed computational fluid dynamics simulation of wind tunnel experiments on natural gas flames using the  $k-\epsilon$  realizable version of the eddy viscosity model; however the results obtained were not compared against experimental measurements of the species and temperature. Lawal et al. [13,14] also used the  $k-\epsilon$  realizable version of the eddy viscosity based turbulence closure models in predicting a methane flame in a cross-flow of air and concluded that it performed better than the other variants of the  $k-\epsilon$  turbulence models, however he too did not compare the predictions with measurements of species. Others researchers have predicted the temperatures, radiation and soot in methane-air cross flow diffusion flames with good agreements with experimental data [15–18]. Studies of cross-flow propane flames have received less attention than methane flames. However, important numerical works have been performed on propane flames among which include the work done by Botros & Brzustowski [19], where the authors numerically investigated the temperatures and radiation from a propane jet diffusion flame. Soot in cross flow propane flames has also been predicted with good agreement with experimental data [20,21]. Propane is a major constituent of gas flares both in the upstream and downstream oil and gas sectors and hence its emissions and combustion characteristics are of importance. It has been very challenging to numerically simulate the wake-stabilized flame in cross-flow. Lifted jet flames have been the topic of research for many years due to its industrial relevance and enormous complexity, and very few works have been done in the public domain for modeling wake-stabilized propane flame in cross-flow. Thus one of the main objectives of the paper is to evaluate partially premixed combustion model in the form that is available in FLUENT and the potential of the Large Eddy Simulation in simulating the propane flame in a cross-flow that is relevant to industrial flares. The present paper contributes to the previous work on the prediction of cross-flow flames by investigating the capabilities of the non-premixed and partially premixed combustion models in conjunction with the Reynolds Stress Model as well as the Large Eddy Simulation technique for predicting temperature and species concentrations in wake stabilized propane flames in a cross-flow of air.

## 2. Experimental details

Numerical predictions in the present work are validated against the experimental work performed by Huang and Yang [9], a brief description of which is as follows. The experiment was performed in a suction type, open circuit wind tunnel which had a test section of dimensions  $30 \times 30 \times 110$  cm. The burner was a stainless pipe of inner diameter  $d_i = 5.0$  mm, outer diameter 6.4 mm and length 250 mm. The pipe was positioned perpendicular to the aluminum floor of the test section and protruded 180 mm into the wind tunnel. The origin was centered at the exit plane of the burner tube and the description was in terms of a rectangular coordinate system (X, Y, Z) as shown in Fig. 1. Commercial grade propane of about 95.0%  $C_3H_8$ , 3.5%  $C_2H_6$  and 1.5%  $C_4H_{10}$  was used as the fuel and the average jet velocity,  $u_j$  was calculated (using the flow rate) to be 5.78 m/s while the fuel Reynolds number was calculated to be about 7000 for the case investigated. The cross-flow velocity  $u_w$  was fixed at 4.86 m/s, giving a jet-to-cross-flow momentum ratio  $R$ , of 2.16. The maximum turbulence intensity of the cross-flow in the wind tunnel section, as measured by a hot-wire anemometer, was less than 0.5% in the experimental range. The thermal structure of the flame was measured with a Pt–Pt/13% Rh home-made L-shaped thermocouple probe with a wire diameter of 125  $\mu$ m and a junction diameter of 150  $\mu$ m mounted on a two-dimensional traversing mechanism. Temperature measurements were not corrected for the radiative losses from the thermocouple and according to the calculation of the energy balance, the deviation of the measured temperature from the actual value was estimated to be about 50 °C at a temperature of 1600 °C. The concentrations of carbon dioxide and carbon monoxide were measured with infra-red analyzers while the concentration of oxygen was measured with a paramagnetic analyzer. Gas sampling was achieved with a stainless steel probe with a tip diameter of about 1 mm.

## 3. Numerical models

Mathematical models available in the commercial CFD software package ANSYS-Fluent 14.0 [22] were used to simulate the combustion. The codes solve the Favre-averaged form of the balance equations for mass, momentum, energy and the relevant scalar quantities describing

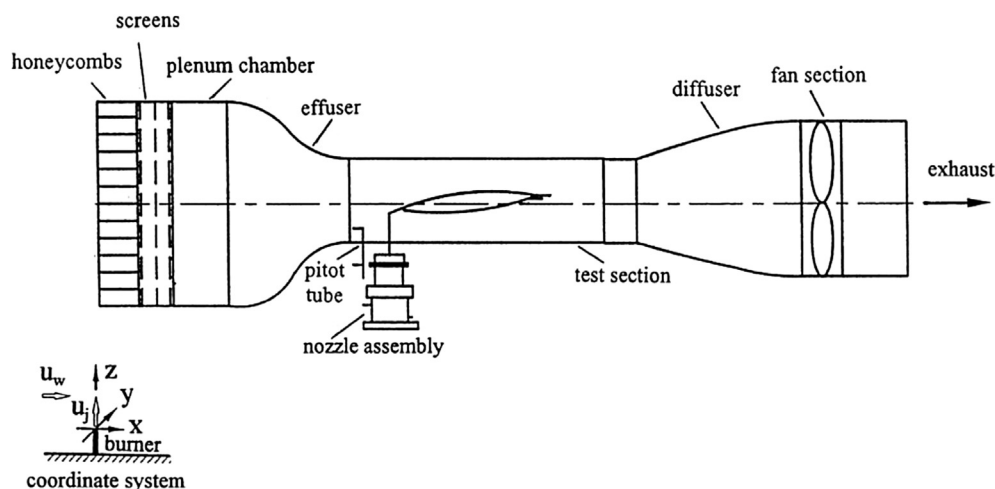


Fig. 1. Wind tunnel set-up of the experiment (based on Ref. [10]).

the turbulence and combustion based on the finite volume solution method. The flow field has been modeled using the Reynolds-Averaged Navier-Stokes (RANS) equations and by the LES technique. The Reynolds stresses arising from the RANS equation are resolved using the Reynolds Stress Model [23]. The combustion was modeled with the laminar flamelet model [24] and also with the partially premixed model with the aim of comparing the capabilities of the two models. Radiation, which appears as a sink in the energy equation, was modeled with the Discrete Ordinate Model [25], and the Moss-Brookes-Hall model [26] was used to simulate the soot formation while the kinetics of the propane reactions were modeled using the CRECK reaction mechanism [27]. The Moss-Brookes-Hall model employed in this paper is an extension to the Moss-Brookes model for higher hydrocarbon fuels. A recent publication with experimental validation showed that the model is suitable for simulating soot formation of heavy hydrocarbon fuels and the model is available in commercial CFD software packages such ANSYS FLUENT and Star-CD. It should be noted though that soot concentrations were not measured in the experiments that are modeled in this paper so it is not possible to compare these results.

### 3.1. Flow models

The Reynolds stress transport Model solves the transport equation for the turbulent or Reynolds stresses directly and this eliminates the need for the turbulent viscosity and the gradient transport theory in the eddy viscosity-based turbulence closure models. In general, the Reynolds-stress model involves the solution of three normal stresses, three shearing stresses and the dissipation rate. The three normal stresses are always solved, but the shearing stresses are solved only when the appropriate velocity components are solved. The exact transport equation for the Reynolds stresses can be derived from the Navier-Stokes equation and it is given as:

$$\frac{\partial}{\partial t} \left( \overline{\rho u_i' u_j'} \right) + \frac{\partial}{\partial x_k} \left( \rho u_k \overline{u_i' u_j'} \right) = D_{ij} + P_{ij} + C_{ij} + \phi_{ij} - \varepsilon_{ij} - F_{ij} \quad (1)$$

where the first and second left hand terms are the transience and convection terms, respectively. The six right hand terms give the diffusion, shear production, buoyancy production, redistribution, dissipation and production by system rotation terms, respectively. The redistribution term, commonly known as the pressure-strain term is the most important term requiring closure. The pressure rate of strain takes the form [28]:

$$\phi_{ij} = \phi_{ij,1} + \phi_{ij,2} + \phi_{ij,w} \quad (2)$$

where the slow part of the pressure rate of strain  $\phi_{ij,1}$  is modeled as:

$$\phi_{ij,1} \equiv -C_1 \rho \frac{\varepsilon}{k} \left[ \overline{u_i' u_j'} - \frac{2}{3} \delta_{ij} k \right] \quad (3)$$

and the rapid part  $\phi_{ij,2}$  is modeled as:

$$\phi_{ij,2} = -C_2 \left[ (P_{ij} + F_{ij} + 5/6 C_{ij} - G_{ij}) - \frac{2}{3} \delta_{ij} (P + 5/6 G - C) \right] \quad (4)$$

where  $\varepsilon$  is the rate of dissipation of turbulent kinetic energy,  $k$  is the turbulent kinetic energy,  $G_{ij}$  is the convection term, and  $P = \frac{1}{2} P_{kk}$ ,  $C = \frac{1}{2} C_{kk}$ , and  $G = \frac{1}{2} G_{kk}$ . The model constants  $C_1$  and  $C_2$  are given as 1.8 and 0.6 respectively [28]. The last term in Eq. (2) is known as the wall reflection term and is responsible for the redistribution of normal stresses near the wall. It is included by default in the Reynolds Stress Model.

In the LES approach, the Navier-Stokes equation is directly resolved in real time for the large scale eddies, however the smaller scale eddies are modeled using a subgrid scale model. Several models are available for approximating the subgrid scale stresses that arise from the filtering operation, and the Smagorinsky model [29] has been widely used with this method being adopted here. The filtering equation is defined such that:

$$\overline{\Delta} G(x - x') = 1 \left| x - x' \right| < \overline{\Delta} = 0 \left| x - x' \right| > \overline{\Delta} \quad (5)$$

where the large eddies which are resolved have filter width  $> \overline{\Delta}$  while the smaller eddies which are discarded and later modeled have filter  $< \overline{\Delta}$ . Applying this mathematical tool to the instantaneous governing equations produces the filtered form. The sub-grid scale stress is given as:

$$\tilde{\tau}_{ij} = \frac{1}{3} \tau_{kk} \delta_{ij} - 2\mu_t \overline{S}_{ij} \quad (6)$$

where  $\mu_t$  is the subgrid – scale turbulent viscosity,  $\tau_{kk}$  is the isotropic part of the subgrid scale stresses (which is not modeled, but added to the filtered static pressure term),  $\overline{S}_{ij}$  the rate-of-strain tensor for the resolved scale and  $\delta_{ij}$  is the Kronecker delta.

### 3.2. Combustion models and reaction mechanism

Non-premixed and partially premixed models have been used to model the combustion. The non-premixed model is based on the concept of a flamelet [24] which considers a turbulent flame as a collection of thin laminar flame structures (flamelets) entrenched within the turbulent flow field. The flamelet theory is built upon certain assumptions, amongst the key ones being that the Lewis number is unity and a common diffusivity is adopted for all species. Furthermore, combustion is assumed to take place near the surface of the stoichiometric mixture in which the reaction zone thickness becomes thinner than the Kolmogorov eddy [30]. The flamelet concept is an extension of the

equilibrium model to include the effect of finite rate chemistry, hence its description includes solving the scalar equation for the mixture fraction. The mixture fraction  $Z$ , is the mass fraction that originated from the fuel stream. The mixture fraction is a conserved scalar quantity and its governing transport equation does not have a source term. Combustion is thus reduced to a mixing problem and the intricacies of closing non-linear mean reaction rates are avoided. If a reactive system is considered to be in a state of chemical equilibrium, then the instantaneous values of the density, temperature and mass fractions depend solely on the instantaneous mixture fraction,  $Z$ , namely

$$\phi_i = \phi_i(Z), \quad \phi = \rho, T, Y_i \quad (7)$$

This is the power of the mixture fraction modeling approach, in that the chemistry is reduced to one or two conserved mixture fractions and under the assumption of chemical equilibrium, all thermochemical scalars (species fractions, density and temperature) are uniquely related to the mixture fraction. For near-equilibrium calculations and non-equilibrium conditions, the steady flamelet and unsteady flamelet approaches are used, respectively. The flamelet equation is given in mixture fraction space as:

$$\rho \frac{\partial Y_i}{\partial t} = \rho \frac{\chi}{2} \frac{\partial^2 Y_i}{\partial Z^2} + \dot{w}_i \quad (8)$$

where  $Y_i$  is species mass fraction,  $\rho$  is density,  $\dot{w}_i$  is species reaction rate and  $\chi$  is the scalar dissipation rate. A similar equation can be written for temperature in mixture fraction space. If time variation is ignored and the left-hand side of Eq. (8) is reduced to zero, then the problem becomes a steady flamelet calculation. The scalar dissipation rate,  $\chi$  accounts for the departure of the flame from equilibrium conditions (i.e. non equilibrium conditions). The scalar dissipation rate controls the mixing and provides the interaction between the flow and the chemistry and it is modeled as:

$$\chi = 2D \left( \frac{\partial Z}{\partial x_j} \right)^2 \quad (9)$$

where  $D$  is the diffusion coefficient of the scalar. Furthermore, the presence of turbulence in the flow field introduces fluctuations in the mixture fraction and in the scalar variables, therefore, the relation between the mixture fraction with the reacting species composition and temperature become nonlinear and can no longer be obtained using Eq. (7). A PDF approach is therefore used to obtain the mean values of the species composition and temperature by weighing their instantaneous relationship with the mixture fraction.

Partially premixed flames exhibit the properties of both premixed and non-premixed flames. They can occur when a diffusion flame becomes lifted so that some premixing occurs prior to combustion. The partially premixed flame can be considered as premixed systems with non-uniform fuel-oxidizer mixtures (equivalence ratios). The partially premixed combustion model employed in this paper is based on the reaction progress variable in combination with the non-premixed flamelet model in order to model the wake-stabilized flame in cross-flow. The premixed reaction-progress variable determines the position of the flame front. Behind the flame front ( $c = 1$ ), the mixture is burnt and the equilibrium or laminar flamelet mixture fraction solution is used. In front of the flame, ( $c = 0$ ), the species mass fractions, temperature and density are calculated from the mixed but unburnt mixture fraction. Within the flame ( $0 < c < 1$ ), a linear combination of the unburnt and burnt mixtures is used. The reaction progress variable unlike the mixture fraction is a non-passive scalar and its transport equation involves a reaction source term. The transport equation of the reaction progress variable is given as:

$$\frac{\partial(\rho\bar{c})}{\partial t} + \frac{\partial}{\partial x_i} (\rho u_i \bar{c}) = \frac{\partial}{\partial x_j} \left[ \frac{\mu_t}{Sc_t} \left( \frac{\partial \bar{c}}{\partial x_j} \right) \right] + \rho S_c \quad (10)$$

where  $\mu_t$  is the turbulent viscosity,  $\bar{c}$  is the mean reaction progress variable,  $Sc_t$  is the turbulent Schmidt number and  $S_c$  is the reaction progress source term. The partially premixed model solves a transport equation for the mean reaction variable  $\bar{c}$  to determine the position of the flame front, as well as a transport equation for the mean mixture fraction  $\bar{Z}$  and the mixture fraction variance  $\overline{Z^2}$ . There are numerous investigations on the partially premixed combustion modeling of lifted jet flames and the models for the reaction rate term in the  $c$ -equation can show some significant impact on the model predictions for the lifted methane jet flames compared with experiments [31,32]. In this paper, the source term of the  $c$ -equation above is calculated as proposed by Zimont et al. [33] linking the reaction rate to the turbulence flame speed. In applying the partially premixed model, the underlying assumptions of the non-premixed and the premixed model applies directly to the partially premixed model.

The kinetics of the chemical reactions was simulated using the CRECK reaction mechanism which contained 113 species and 1909 reactions. The mechanism is highly detailed and is designed to handle the high temperature pyrolysis, partial oxidation and combustion of hydrocarbon fuels with up to three carbon atoms. Ranzi et al. [27] have reviewed several successful applications of the mechanism to the modeling of hydrocarbon and oxygenated fuels such as alkanes, alkynes and alcohols. The mechanism was implemented in the CHEMKIN format and it took about 24 h to generate a flamelet library in the fluent solver using the mechanism. Apart from the turbulence–chemistry interaction, the combustion chemistry presents the most difficult challenge in the modeling of combustion processes; hence it is important that the mechanism must be as detailed as possible involving a possible minimum number of species in order to make the calculations more tractable. A further advantage of the mechanism is that it is also applicable to hydrocarbon fuel mixtures making it suitable for combustion processes in which commercial grade propane is used as the fuel, as is the case in the present simulation.

### 3.3. Soot and radiation model

Soot in the flames was modeled using the Moss-Brookes-Hall model [26] as implemented in the Fluent code, in which soot nucleation and growth are based on acetylene ( $C_2H_2$ ) as the soot precursor and gas phase specie. Soot oxidation is based on the model by Lee et al. [34] which accounts for soot oxidation by both [O] and [OH] species in addition to  $O_2$  oxidation. Soot formation and soot oxidation are competing

processes in a flame and the amount of soot emitted will depend on the balance between these two processes. These processes can be expressed mathematically as:

$$\frac{dM}{dt} = \left(\frac{dM}{dt}\right)_{Inc.} + \left(\frac{dM}{dt}\right)_{Gro.} + \left(\frac{dM}{dt}\right)_{Oxid.} \quad (11)$$

where  $M$  represents the soot mass density, the first and second right-hand terms represent rates of soot formation (inception and growth) and the third term represents the rate of soot oxidation. The Moss–Brookes–Hall model is two equation model which uses the soot particle number density  $N$ , in addition to the soot mass density to formulate the soot equations. Ethylene ( $C_2H_4$ ) was selected as a gas phase species given its prevalence in the propane reaction mechanism. This approach has been demonstrated by Wen et al. [35] where they used a combination of acetylene ( $C_2H_2$ ) and benzene ( $C_6H_6$ ) as soot precursors to model soot in kerosene flames. In the soot inception models used by Brookes and Moss, the rate of change of soot mass density is related to soot number density by the equation:

$$\left(\frac{dM}{dt}\right)_{Inc.} = \frac{M_p}{N_A} \left(\frac{dN}{dt}\right)_{Inc.} \quad (12)$$

where  $M_p$  is the mass of a soot nucleus with a value of 1200 kg/mol and  $N_A$  is the Avogadro's number. The acetylene inception model [36] is founded upon the simplifying assumption that soot inception is a first order function of the acetylene concentration. Based on the pyrolysis equation of acetylene, given as:



The soot inception rate is given as:

$$\left(\frac{DN}{dt}\right)_{Inc.} = c_1 N_A \left(\rho \frac{Y_{C_2H_2}}{W_{C_2H_2}}\right) e^{-\frac{21100}{T}} \quad (14)$$

where  $c_1 = 54 s^{-1}$  as determined by Brookes and Moss and the activation temperature was proposed by Lindstedt [36]. Hall et al. [26] gave an expression for the soot inception rate based on the presence of polyaromatic hydrocarbons in the gas phase as:

$$\left(\frac{DN}{dt}\right)_{Inc.} = 8 \cdot c_2 \frac{N_A}{M_p} \left[\rho^2 \left(\frac{Y_{C_2H_2}}{W_{C_2H_2}}\right)^2 \frac{Y_{C_6H_5} W_{H_2}}{W_{C_6H_5} Y_{H_2}}\right] e^{-\frac{4378}{T}} + 8 \cdot c_3 \frac{N_A}{M_p} \left[\rho^2 \frac{Y_{C_2H_2} Y_{C_6H_6} Y_{C_6H_5} W_{H_2}}{W_{C_2H_2} W_{C_6H_6} W_{C_6H_5} Y_{H_2}}\right] e^{-\frac{6390}{T}} \quad (15)$$

where  $c_2 = 127 \times 10^{8.88}$  and  $c_3 = 178 \times 10^{9.50}$ , as determined by Hall et al. [26]. The soot oxidation term due to oxygen and the hydroxyl radical are given as [34]:

$$\left(\frac{dM}{dt}\right)_{Oxid.} = -C_{oxid} C_{\omega,1} \eta_{coll} \left(\frac{X_{OH} P}{RT}\right) \sqrt{T} (\pi N)^{1/3} \left(\frac{6M}{\rho_{soot}}\right)^{2/3} - C_{oxid} C_{\omega,2} \eta_{coll} \left(\frac{X_{O_2} P}{RT}\right) \exp\left\{\frac{T_{\omega,2}}{T}\right\} \sqrt{T} (\pi N)^{1/3} \left(\frac{6M}{\rho_{soot}}\right)^{2/3} \quad (16)$$

where the collision efficiency  $\eta_{coll}$  is given as 0.13, the oxidation rate scale parameter  $C_{oxid}$  is taken to be unity, the constants  $C_{\omega,1}$  and  $C_{\omega,2}$  are taken to be 105.81 and 8903.51 kg m kmol<sup>-1</sup> K<sup>-1/2</sup> s<sup>-1</sup> respectively and  $T_{\omega,2}$  is given as 19778 K [26].

The Discrete Ordinate model [25] that is available in FLUENT was used to account for the radiant heat from the flames. The model is able to account for both the absorption and the emission of radiation. The effect of the soot on radiation was taken into account by including the effect of the soot concentration on the radiation absorption coefficient. The soot absorption is calculated using:

$$a_s = b_1 \rho_m [1 + b_T (T - 2000)] \quad (17)$$

where  $\rho_m$  is the soot density in kg m<sup>3</sup>, and  $b_T$  and  $b_1$  are the coefficients obtained from a curve to the fitted experimental data [37].

#### 4. Computational details

The computational simulation was achieved on a three-dimensional structured hex mesh generated using the ANSYS-ICEM meshing software which in general produces more accurate solutions with less number of computational cells. The size of the computational domain was based on the volume of the test section of the wind tunnel ( $30 \times 30 \times 110 \text{ cm}^3$ ) with the origin at the center of the burner outlet to reduce the influence of the upper and lower boundary of the computational domain. The burner was represented by a cylindrical tube with dimensions consistent with that used in the experimental set up. The tube was positioned approximately 240 mm from the cross-flow inlet boundary and it extended 180 mm into the combustion zone so that the influence of the flare-pipe on the flow at the inlet boundary is minimized and also, a fully developed flow may be assumed in the downstream boundary. A mesh independent study was conducted (for the RANS calculations) to ensure the independence of the solution on the mesh size, and a mesh density of 2.52 million cells was found to suffice (see Fig. 2). The mesh distribution option was selected so as to place a finer node distribution in the pipe region in order to resolve the interaction between the pipe and the flow. Using the RSM turbulence model often pose convergence problems in RANS simulations. Investigation has shown that calculations using the RSM converged faster when started from a converged solution using the  $k-\epsilon$  realizable turbulence model. Likewise, in order to increase the stability of the calculations, the reacting flow simulation was started from a converged solution of a non-reacting flow. Further, a total number of 16 flamelets over a scalar dissipation rate 0.0001 s–30 s<sup>-1</sup> in scalar dissipation steps of 2.5 s<sup>-1</sup> have been employed, which has been shown to give adequate accuracy for the case considered [14].

The LES calculation was performed in time step sizes of  $1.2 \times 10E-4$ , for a flow time of 1.40 s in order to achieve a pseudo-steady state solution. This is approximately 2 flow residence times through the solution domain and the cell courant number had stabilized at around 1.5 at the end of the calculations and all iteration residuals were observed to be below  $10^{-6}$ . The Smagorinsky-Lily model [29] was used to



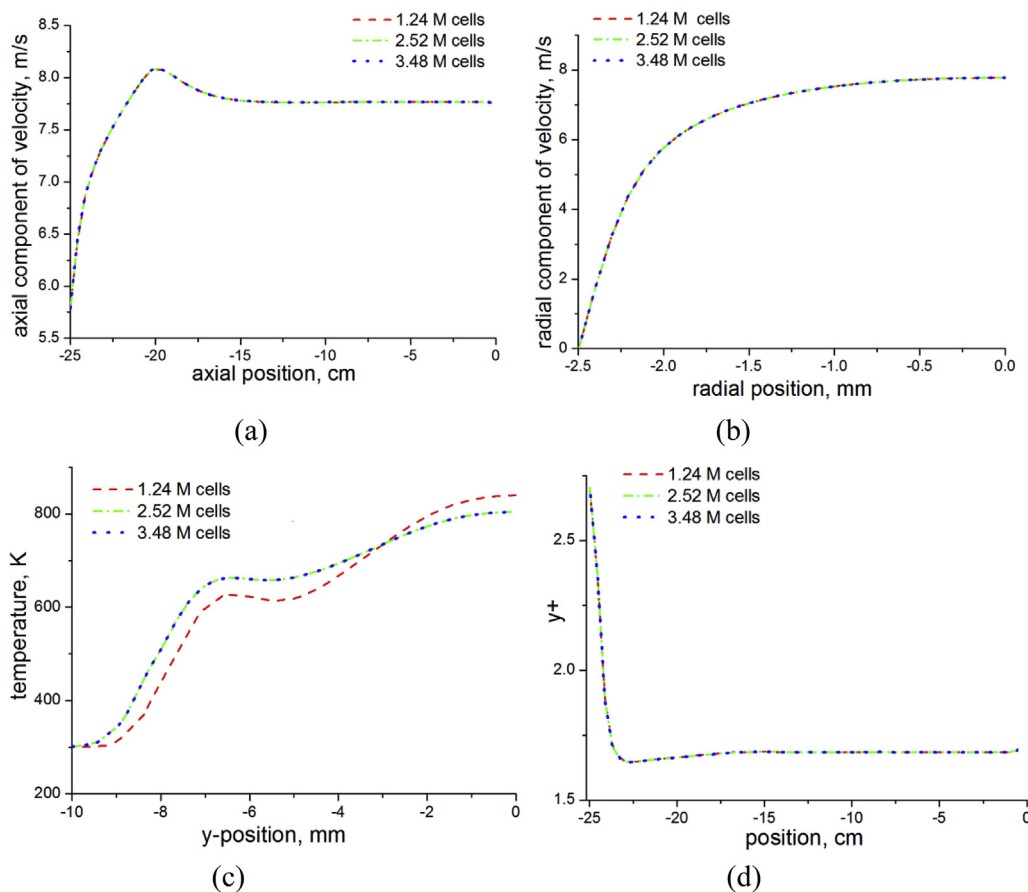


Fig. 2. Predictions of (a) axial, (b) radial velocity, (c) temperature at  $x = 8.2, z = 3$  mm, and (d) pipe wall  $y^+$  for 1.24, 2.52, and 3.48 M cells for  $Re = 7000$ .

approximate the sub-grid scale turbulence in the flow domain while the kinetics of the propane reactions was accounted for using the CRECK reaction mechanism of Ranzi et al. [27]. All governing equations were discretized using the second-order upwind scheme and the pressure–velocity coupling was resolved by the SIMPLE algorithm [38] as implemented in the FLUENT code. To achieve convergence, trial and error were carried out to correct the floating point errors in the solver. To this end, the under-relaxation factors were decreased midway into the calculation to avoid divergence in the AMG solver. This is because over relaxation speeds up the convergence, but at the same time will reduce the calculation stability. This also necessitated a switch of the pressure–velocity coupling discretization technique from SIMPLE to Coupled solver in order to stabilize the LES calculation. The SIMPLE algorithm solves the momentum and continuity equations in a segregated manner and the coupled algorithm solves the momentum and continuity equations together [38]. Boundary conditions have been prescribed as follows: on the  $z-x$  plane, a no-slip wall boundary condition was specified at the front and back of the box. On the  $z-y$  plane, corresponding to the cross-flow inlet, a uniform velocity profile and 0.18% turbulence intensity was specified. Downstream of this plane, outflow conditions were implemented where a zero value of the normal gradient for all flow variables, except pressure, were specified. At the pipe inlet, a uniform fuel velocity was specified with a 10% turbulence intensity which is representative of the fully developed flow in the pipe. No-slip wall boundary conditions were implemented at the pipe walls. Stationary and no-slip wall boundary conditions were also specified on the  $z-x$  planes, representing the box enclosure. Similar conditions were also implemented at the top and bottom of the box corresponding to the  $x-y$  planes. For Large Eddy Simulation, the mixture fraction variance was employed for calculating the non-premixed flamelets, and thus the mean scalar dissipation is modeled with a gradient approach with a dynamically calculated constant, instead of solving the transport equation as in the RANS model. In addition, care has been taken to ensure that the mesh employed for the LES simulation resolves most of the large scale turbulence. However, for the regions near to the wall of the flare-pipe where the mesh is not fine enough to resolve the laminar sublayer, the near-wall treatment based on Werner and Wengle [39] was employed.

## 5. Results and discussion

### 5.1. Flame structure

Studies of wake-stabilized propane flames in a cross-flow of air have revealed a three-zone flame structure made up of a recirculating eddy attached to the lee-side of the pipe, a mixing layer of non-reacting fuel from the pipe carried over the eddy, and an axisymmetric main tail of the flame [7]. This behavior in the flame has been captured by the Reynolds Stress turbulence Model as shown in Fig. 3(a) and (b), where the low pressure region and the recirculation zone can be seen, respectively. In this flow regime, the momentum of the cross